Macromolecules
ARTICLE

Macromolecules **2010**, *43*, 8045–8050 **8045**
DOI: 10.1021/ma101657e

Impact of Pendant 1,2,3-Triazole on the Synthesis and Properties of Thiophene-Based Polymers

G. Nagarjuna, Serkan Yurt, Kedar G. Jadhav, and D. Venkataraman*

Department of Chemistry, University of Massachusetts Amherst, 710. N. Pleasant Street, Amherst, Massachusetts 01003

Received July 23, 2010; Revised Manuscript Received August 31, 2010

ABSTRACT: π-Conjugated moieties are often attached to conjugated polymers to systematically alter their electronic properties. Herein, we report the synthesis and properties of a thiophene polymer bearing a triazole moiety in the third position. Through NMR-based quenching studies, we show that the placement of the triazole moiety alters reaction pathway of the Ni(0)-mediated Grignard metathesis polymerization possibly through chelation. When compared with a triazole on the main chain, the pendant triazole moiety acts as an electron donor and lowers the band gap of the polymer. The triazole moiety also does not hinder the packing of the conjugated backbone. We also show that the fluorescence of this polymer is quenched with PCBM, indicating its potential as a candidate for organic photovoltaic devices.

Introduction

Functionalization of conjugated polymers with π-conjugated side chains is receiving widespread attention to create next generation active materials for organic-based devices such as sensors, field effect transistors, and photovoltaic devices because of their high mobility and the presence of broad absorption bands in the UV−vis spectra.[1−14] 1,3-Dipolar cycloaddition[15] is widely used for the functionalization of polymers in general[16,17] and conjugated polymers in particular.[18−21] In all these cases, there is a nonconjugated spacer between the polymer backbone and triazole. We reasoned that the placement of the triazole moiety in conjugation with a monomer such as thiophene through 1,3-dipolar cycloaddition reaction may offer a convenient pathway to append π-conjugated moieties to the conjugated polymer backbone and systematically alter the electronic properties of the conjugated polymer. Herein, we show that the polymerization of the monomer with the triazole moiety at the third position of thiophene through Ni(0)-mediated Grignard metathesis polymerization reaction is not straightforward. The triazole moiety reverses the typical selectivity of Grignard metathesis in 2,5-dibromothiophene-based systems and stops the polymerization reaction. We show that this problem can be overcome and report in here a protocol for the synthesis of thiophene-based polymers bearing a triazole moiety at the third position. We also present the impact of the triazole moiety on the optical properties of the polymer.

Experimental Section

UV−vis absorption spectra were recorded with a Shimadzu UV 3600PC spectrometer in Polymer-Based Materials Harvesting Solar Energy (Energy Frontier Research Center at the University of Massachusetts Amherst) EFRC laboratory. Stock solutions of polymers (c = 1 mg/10 mL) were prepared in spectrophotometric grade chloroform (Fisher, Optima). UV−vis experiments for thin films were done by spin-casting (1400 rpm, 60 s) 1 wt % solution of polymer in chloroform on a glass plate. Similarly to the 1 wt % solution of polymer in chloroform, phenyl-C_{61}-butyric acid methyl ester (PCBM) (1:1 wt % with respect to polymer) was added and spun-cast (600 rpm) onto a glass plate. These films were annealed at 100 °C for 30 min. UV−vis and fluorescence spectra were recorded before and after annealing. Fluorescence spectra were measured on PTA fluorimeter for thin films and on a JASCO FP-6500 spectrofluorometer for solution studies. Cyclic voltammetry studies were done using a BAS CV-50 W instrument. Stock solutions of polymer (1 wt % polymer in chloroform) were prepared, films were drop-cast on to the platinum working electrode, and CV was recorded with tetrabutylammonium hexafluorophosphate as a supporting electrolyte (0.1 M) in acetonitrile. The redox potentials were determined against $Ag/AgNO_3$ reference electrode. In these conditions, the redox potential of Fc/Fc^+ (Fc = ferrocene) was +0.09 V versus Ag/Ag^+. It is assumed that the redox potential of Fc/Fc^+ has an absolute energy level of −4.80 eV to vacuum.[22−24] HOMO and LUMO values were calculated using Fc/Fc^+ as a reference. The working and auxiliary electrodes were cleaned after each run. Synthetic protocols for hitherto unknown molecules **1**, **4**, **M1**, and **M2** are discussed here. Synthetic protocols for all other molecules are provided in the Supporting Information.

3-Iodothiophene (1). A Schlenk tube was charged with CuI (0.70 g, 3.68 mmol) and NaI (22.0 g, 147.2 mmol) under a nitrogen atmosphere. Xylene (57.6 mL) and diglyme (14.4 mL) were added followed by the addition of the ligand *N*,*N*-dimethylethylenediamine (0.79 g,7.36 mmol). Finally, 3-bromothiophene (12 g, 73.6 mmol) was added under a nitrogen atmosphere. The Schlenk tube was sealed with a Teflon valve, and the reaction mixture was stirred at 110 °C for 22−24 h. The resulting suspension was allowed to reach room temperature. The solvents xylene and diglyme were removed under reduced pressure, and the resulting mixture was extracted with hexanes (2 × 75 mL). The combined organics were washed with water (1 × 75 mL) and saturated NaCl solution (1 × 75 mL), dried over Na_2SO_4, and concentrated, and the residue was purified by silica gel chromatography (hexanes) to provide **1** as a yellow liquid (12.3 g, 80%). ^{1}H NMR (400 MHz, $CDCl_3$): δ 7.41 (dd, J = 4.8, 3.0, 1H), 7.21−7.19 (m, 1H), 7.11−7.09 (dd, J = 4.8, 1H). ^{13}C NMR (100 MHz, $CDCl_3$): δ 134.74, 128.65, 127.34, 77.20.

4-(2,5-Dibromothiophen-3-yl)-1-hexyl-1*H*-1,2,3-triazole (M1). To an oven-dried round-bottom flask was added CuI (0.472 g,

*Corresponding author. E-mail: dv@chem.umass.edu.

Published on Web 09/20/2010

2.48 mmol) and THF (50 mL). To this stirred solution, *N*,*N*-diisopropylethylamine (3.845 g, 29.81 mmol) and water (10 mL) were added followed by the addition of monomer (2,5-dibromothiopen-3-ylethnyl)trimethylsilane (**3**) (1.68 g, 4.96 mmol) and 1-azidohexane (0.947 g, 7.45 mmol). The reaction was stirred for 15 h under reflux conditions and quenched with water. The layers were separated, and the aqueous layer was extracted with ethyl acetate (2 × 50 mL). The combined organics were washed with brine (2 × 50 mL), dried over Na_2SO_4, filtered, and concentrated under reduced pressure. Purification of the residue by silica gel chromatography (20:80 EtOAc: hexanes) afforded **M1** as a white solid (1.37 g, 70%). ^{1}H NMR (400 MHz, $CDCl_3$): δ 8.13 (s, 1H), 7.64 (s, 1H), 4.42 (t, J = 7.0, 2H), 1.98−1.91 (m, 2H), 1.37−1.29 (m, 6H), 0.90 (t, J = 7.0, 3H). ^{13}C NMR (100 MHz, $CDCl_3$): δ 141.03, 132.61, 131.35, 120.65, 112.52, 107.02, 50.58, 31.14, 29.72, 26.15, 22.43, 13.96. MS (FAB+) m/z 393.9 $[M + H]^+$.

2-Bromo-3-iodothiophene (4). In the absence of light, NBS (7.8 g, 49.22 mmol) was added in one portion to a stirred solution of **1** (8.1 g, 44.74 mmol) in DMF (200 mL). After stirring at room temperature for 12 h, the reaction was quenched with water (200 mL) and extracted with hexanes (2 × 75 mL). The combined organics were washed with brine (2 × 75 mL), dried over Na_2SO_4, filtered, and concentrated under reduced pressure. Purification of the residue by silica gel chromatography (hexanes) afforded **4** (8.35 g, 75%) as a pale yellow liquid. ^{1}H NMR (400 MHz, $CDCl_3$): δ 7.22−7.24 (d, J = 5.6, 1H), 6.95−6.96 (d, J = 5.6, 1H) ^{13}C NMR (75 MHz, $CDCl_3$): δ 137.08, 116.31, 113.46, 85.21.

4-(2-Bromo-5-iodothiophen-3-yl)-1-hexyl-1*H*-1,2,3-triazole (M2). Compound **6** (1.6 g, 5.091 mmol) was dissolved in dichloromethane. To this solution, trifluoromethanesulfonic acid (3.82 g, 25.45 mmol) was added and the solution cooled to 0 °C using an ice bath. *N*-Iodosuccinimide (1.15 g, 5.091 mmol) was added in small portions, and the reaction mixture was stirred for 12 h at room temperature. The reaction mixture was quenched with ice water and extracted with CH_2Cl_2 (3 × 25 mL). The combined organic extracts were washed with aqueous 10% sodium bisulfate solution, dried over sodium sulfate and the solvent was removed under reduced pressure. The residue was purified by silica gel chromatography (15% ethyl acetate/hexane) to provide **M2** as a white powder. ^{1}H NMR (400 MHz, $CDCl_3$): δ 8.15 (s, 1H), 7.85 (s, 1H), 4.42 (t, J = 7.0, 2H), 1.98−1.91 (m, 2H), 1.37−1.29 (m, 6H),0.90(t, J = 7.0,3H). ^{13}C NMR (100 MHz, $CDCl_3$): δ 140.84, 137.63, 133.85, 120.61, 110.84, 72.68, 50.70, 31.27, 30.42, 26.28, 22.56, 14.09.

Quenching Studies. M1 (134 mg, 0.340 mmol) was dissolved in THF and transferred into a Schlenk flask under an argon atmosphere. *tert*-Butylmagnesium chloride (0.22 mL, 0.374 mmol) was added via syringe, and the reaction mixture was stirred at room temperature for 2 h. It was then quenched with water and extracted with diethyl ether (3 × 25 mL). The combined organic extracts were washed with brine and dried over sodium sulfate and evaporated under reduced pressure. ^{1}H NMR was recorded without further purification (Figure 1). The **M2** was also subjected to same reaction conditions as **M1**, except that the Schlenk was cooled to 0 °C throughout the reaction. Workup for **M2** was the same as **M1**, and ^{1}H NMR was recorded without further purification (Figure 1).

Results and Discussion

Synthesis of Polymer and Halogen−Magnesium Exchange Studies. We chose to synthesize (poly(3-(1-hexyl-1*H*-1,2,3-triazole-4-yl)thiophene)), P3TzT, as this polymer would allow us to understand the impact of triazole on the electronic properties of the polythiophene backbone by comparing it with poly(3-hexylthiophene) (P3HT), which is commonly used in organic electronic devices such as photovoltaic cells.[25−31] We synthesized the monomer from readily available 3-bromothiophene,

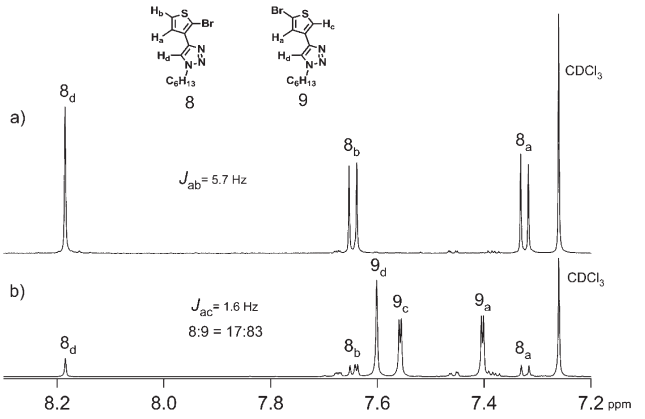

Figure 1. NMR of products obtained after reacting (a) **M2** and (b) **M1** with Grignard and then quenching with water.

which was converted to 3-iodothiophene (**1**) using the Finkelstein reaction.[32] Dibromination of 3-iodothiophene followed by the Sonogashira coupling with trimethylsilylacetylene and 1,3-dipolar cycloaddition with 1-azidohexane gave **M1** in good yields (Scheme 1). We then subjected **M1** to standard Ni(0)-mediated Grignard metathesis polymerization (GRIM) condition.[33,34] When the reaction mixture was poured into methanol (see Supporting Information), no precipitate was obtained, indicating the absence of polymeric products. We did not obtain a precipitate irrespective of whether the polymerization was done at room temperature or at elevated temperatures for 24 h. We hypothesized that the failure of the polymerization may be either due to the inability of **M1** to undergo Grignard metathesis or the inability of the Grignard formed from **M1** to undergo Ni(0)-mediated polymerization or both.

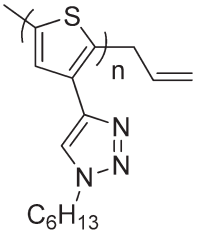

P3TzT

To probe whether **M1** undergoes Grignard metathesis or not, we reacted **M1** with *t*-BuMgCl for 2 h and the reaction mixture was quenched with H_2O (Scheme 2). The organic components were extracted with diethyl ether, and the solvent was removed under reduced pressure. The ^{1}H NMR of residue showed that ratio of the regioisomers was 17:83. For peaks attributable to the product, each peak between δ 7.4 and 7.6 integrated to one proton consistent with a single component with three aromatic protons. On the basis of precedence, the peaks around δ 7.4−7.6 were assigned to protons on thiophene, and the peak at δ 7.6 was assigned to the triazole proton. The coupling constant, J, of the peaks between δ 7.4 and 7.6 was found to be 1.6 Hz, consistent with a "meta" coupling.[35] We therefore concluded that the Grignard metathesis occurred with −Br group at the second position, *ortho* to the triazole moiety (Figure 1). The driving force for the formation of Grignard at this position may be due to the coordination of the triazole nitrogen and the monomer acting as a chelating ligand for Mg^{2+}.

Although there are few reports indicating that the Grignard metathesis at the second position does result in polymerization,[36,37] our result is consistent with earlier

Scheme 1. Synthesis of P3TzT and the Trimer 7

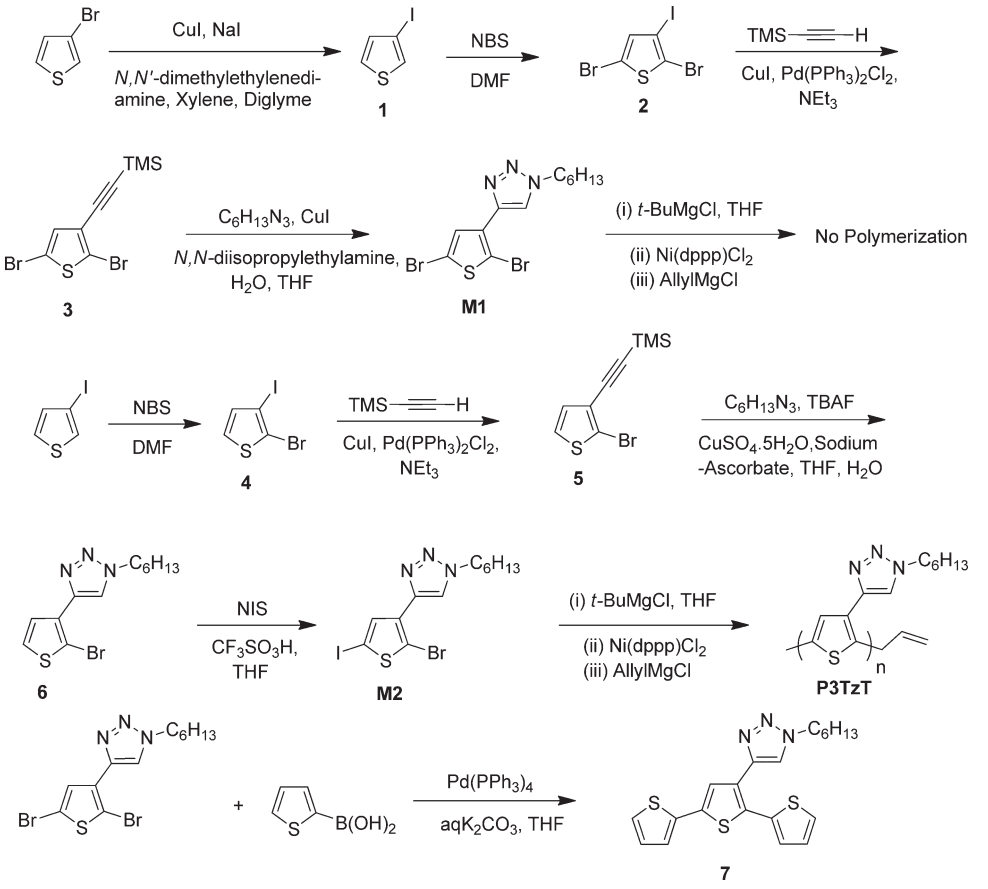

Scheme 2. Quenching Studies for Monomers 1 and 2

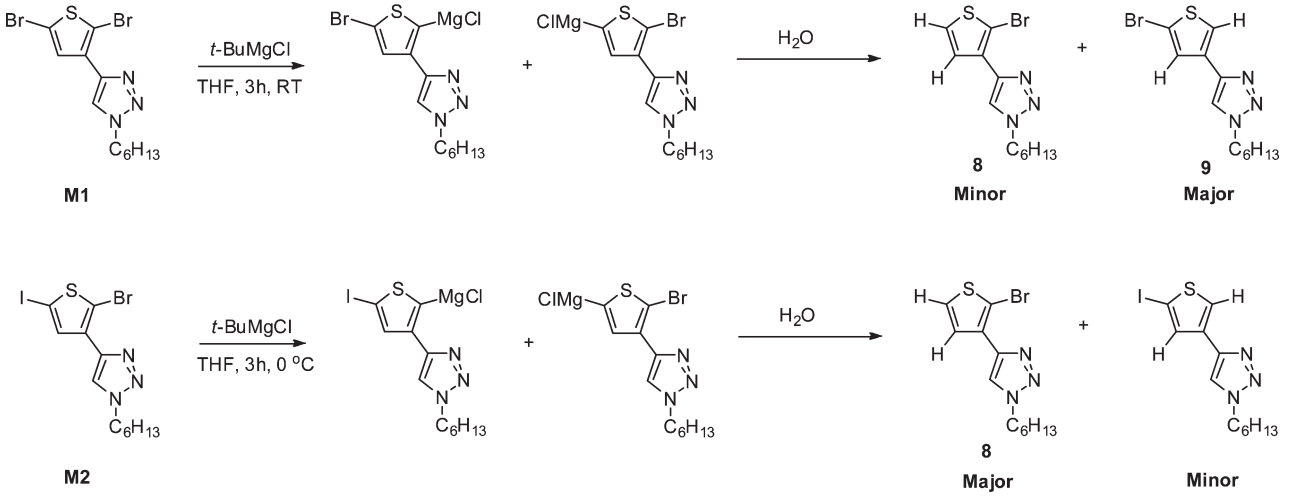

studies[38,39] with 5-bromo-2-iodo-3-hexylthiophene, which have shown that the metal−halogen exchange at second position does not result in polymerization. It has been argued that if the Grignard metathesis occurs at second position on the thiophene ring, then the Ni(0) does not insert in the carbon−bromine bond at the fifth position purportedly due to lack of stabilization from the alkyl chain at the third position. We believe that in our case, since the hexyl group is away from the reaction side, the chelating ability of the triazole moiety may stabilize the Grignard or the nickel(II) complex that results from the Grignard and may prevent further reaction.

To direct the Grignard metathesis at the fifth position of the thiophene, we designed **M2** with iodine at the fifth position and bromine at the second position. Since it is known that Grignard metathesis occurs faster with a C−I than a C−Br bond, we expected that the Grignard reagent should preferentially react at the fifth position. The synthesis of **M2** is shown in Scheme 1. We screened a variety of iodination conditions and found that *N*-iodosuccinimide and trifluoromethanesulfonic acid (NIS/CF_3SO_3H) provided the iodinated compound in excellent yields. **M2** was reacted with *t*-BuMgCl, and the reaction mixture was quenched with water. The coupling constant in the peaks

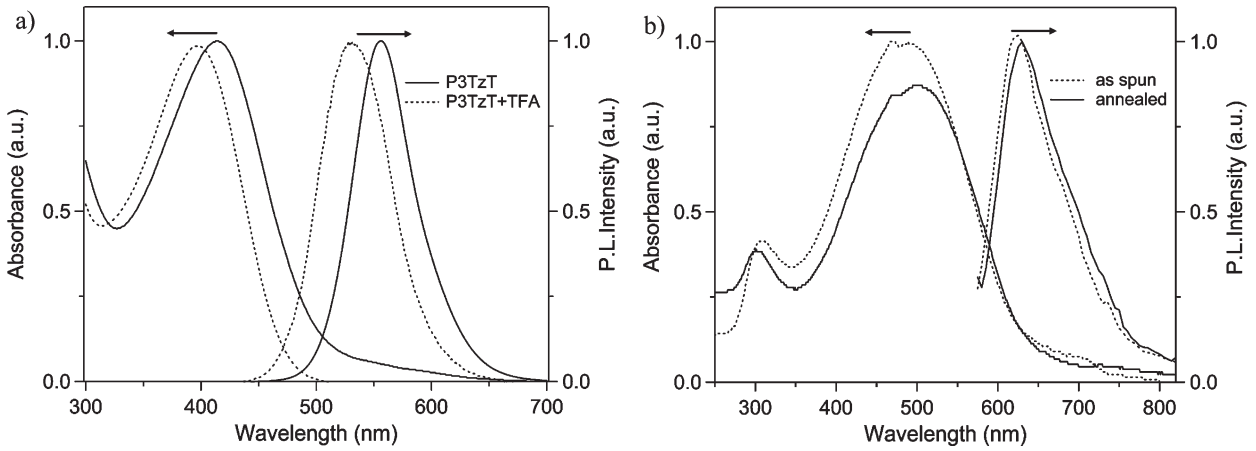

Figure 2. UV−vis absorption and fluorescence spectra of (a) P3TzT in chloroform before and after addition of trifluoroacetic acid (TFA) and (b) P3TzT film before and after annealing.

Table 1. Optical and Electrochemical Data of Polymers[a]

polymer	λ_{max}^{sol} [nm]	λ_{max}^{film} [nm]	E_g^{opt} [eV]	HOMO [eV]	$LUMO^{opt}$ [eV]	$LUMO^{elec}$ [eV]	E_g^{elec} [eV]
P3HT	449	564	1.83	−4.99	−3.16		
P3TzT	415	506	1.90	−4.97	−3.07	−2.94	2.03
P3TzT + TFA	395			−5.02		−2.78	2.24
4RTaz/Th[b]	353	375	2.61	−5.37	−2.76	−2.80	2.57
2D-PT[b]	460	492	1.98	−5.46	−3.48		

[a] E_g^{opt} calculated from the intersection of tangent on the low energetic edge of the absorption spectrum with baseline, HOMO and $LUMO^{elec}$ are calculated from oxidation and reduction potentials obtained from cyclic voltammetry, $E_g^{elec} = LUMO^{elec} - HOMO$, $LUMO^{opt}$ calculated using the equation HOMO + E_g^{opt}. [b] Data are taken from the refs 2, 46, and 47.

between δ 7.3 and δ 7.7 was found to be 5.7 Hz, consistent with the coupling expected between the protons at the fourth and fifth position; this observation is consistent with the metathesis happening at the fifth position (Figure 1).[35] We were gratified to note that **M2** polymerized under GRIM conditions. The polymer (P3TzT, M_n = 24.7 kDa, PDI = 1.48) is soluble in chloroform at room temperature and in DMF at elevated temperature (see Supporting Information).

UV−vis Absorption and Fluorescence Spectra. In the literature, it has been shown that 1,2,3-triazole can act as an electron donor[40] or as an electron acceptor.[41] If triazole acts as electron donor, then we expect that the HOMO levels will be affected whereas if triazole acts as an acceptor, LUMO levels of the conjugated polymer backbone will be affected.[42−45] The resonance and inductive effects of triazole will also depend on the orientation of the triazole ring with respect to the backbone. Therefore, the question is what is the impact of triazole on the electronic structure of the conjugated polymer backbone and on the frontier energy levels?

The UV−vis absorption and fluorescence spectra of the polymer solution and thin film are shown in Figure 2. Solution state UV−vis and fluorescence spectra were recorded using a solution of the polymer in chloroform. Thin films for solid state measurements were cast from chloroform onto a glass slide, and the UV−vis and fluorescence spectra were recorded before and after thermal annealing at 100 °C for 30 min. There was no substantial change in absorption and emission spectra before and after thermal annealing, indicating that no substantial changes occurred in the packing of molecules upon annealing. The absorption λ_{max} in solution is 415 nm and in thin film is 506 nm with a red shift of 91 nm in thin films. In comparison, P3HT has a red shift of 115 nm in thin films. Crystal structures of **M1** and terthiophene (**7**) bearing the triazole moiety show that the triazole is twisted with respect to the thiophene backbone with a dihedral angle of 32° and 45°, respectively (see Supporting Information). Powder X-ray diffraction analysis of the polymer thin film shows peaks at 2.75, 1.52, 0.5, and 0.38 nm, indicating that the polymer is crystalline (see Supporting Information). Even though the crystal structures indicate that the triazole moiety may not be coplanar with thiophene backbone, the noncoplanarity seems to not hinder the packing of the polymer in thin films.

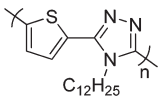

4RTaz/Th

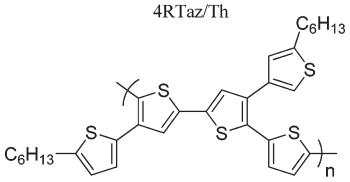

2D-PT

In order to understand the placement effect of triazole in side chain compared to main chain, we compared P3TzT with the polymer reported in the literature, 4RTaz/Th.[46,47] We find that in solution λ_{max} of P3TzT absorption is red-shifted by 62 nm compared to λ_{max} of 4RTaz/Th (see Table 1). The red shift in the solution absorption λ_{max} of P3TzT compared to 4RTaz/Th indicates that the conjugation length has increased, and the band gap of P3TzT is lower compared to 4RTaz/Th (Table 1). Therefore, we believe that 1,2,3-triazole attached as a side chain in P3TzT increases the conjugation and electron density on polymer better than 1,2,4-triazole introduced in the main chain. To understand the effect of triazole versus thiophene as a side chain on the thiophene backbone, we compared P3TzT with the reported polymer, 2D-PT.[2] The thin film absorption λ_{max} of all the

polymers—4RTaz/Th, 2D-PT, and P3TzT—are blue-shifted compared to P3HT. However, the λ_{max} for P3TzT is much closer to P3HT than 4RTaz/Th or 2D-PT. The red shift in λ_{max} of all the polymers from solution to thin film is in the following order: P3HT > P3TzT > 2D-PT > 4RTaz/Th. From the onset absorption values, the band gaps of P3TzT, 4RTaz/Th, and 2D-PT were calculated to be 1.9, 2.61, and 1.98 eV, respectively. It is noteworthy that the absorption λ_{max} of P3TzT in the solution is blue-shifted compared to 2D-PT. Nonetheless, in thin films, the absorption maxima are close. There is a 91 nm red shift in P3TzT absorption from solution to thin film absorption, whereas 2D-PT shows only a 30 nm red shift. Since the red shifts in thin films are related to polymer packing and interaction between the polymer chains, we speculate that triazole facilitates better packing in thin films in P3TzT than conjugated side chains in 2D-PT. We had anticipated that the interaction between the polymer chains in this films will be poor in P3TzT because it has 1,2,3-triazoles on every repeat unit and the triazole ring is not coplanar with the polymer backbone. We therefore conclude that 1,2,3-triazole as a side chain also provides better $\pi-\pi$ interactions between polymer chains in thin films compared to that of thiophene side chains.

The solution and thin film emission λ_{max} of P3TzT are found to be 556 and 630 nm, respectively. The Stokes shift for the solution and thin film are calculated to be 141 and 124 nm, respectively. The higher Stokes shift in P3TzT indicates a higher degree of structural reorganization in P3TzT, which might be facilitated by the conjugated triazole side chains.

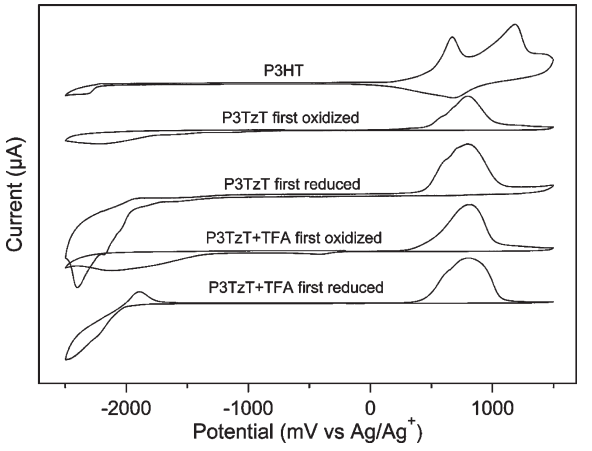

Figure 3. Cyclic voltammograms of P3TzT with and without trifluoroacetic acid (TFA).

Electrochemical Properties and the Nature of Triazole Interaction. P3TzT thin films were drop-cast from a chloroform solution on to the Pt electrode and the oxidation/reduction potentials obtained from the cyclic voltammogram were compared with P3HT. The CV of P3TzT thin film was recorded in two ways: (i) by oxidizing the polymer (positive potential sweep); (ii) by first reducing the polymer (negative potential sweep) (Figure 3). Since the oxidation and reduction of P3TzT are not completely reversible, the onset oxidation and reduction potentials from Figure 3 were used to calculate the HOMO and LUMO^{elec} energy levels (eq 1).

$$\text{HOMO} = -e(E_{ox}^{onset} + 4.71)\ (\text{eV})$$
$$\text{LUMO}^{elec} = -e(E_{red}^{onset} + 4.71)\ (\text{eV}) \quad (1)$$

The onset oxidation and reduction potentials of P3HT and P3TzT are 0.286, −2.18 V and 0.266, −1.766 V, respectively, with respect to Ag/Ag^+. The HOMO, LUMO energy levels and electrical band gaps of P3HT, P3TzT, 4RTaz/Th, and 2D-PT are shown in Table 1 for comparison. The HOMO levels of all the polymers, except P3TzT, are lower than P3HT. In 2D-PT, both the HOMO and LUMO^{opt} levels are lower in energy compared to P3TzT, but both the polymers have very close band gap (E_g^{opt}).

The electrochemical and UV−vis spectroscopic data are consistent with the fact that triazole is behaving as an electron donor instead of an electron acceptor. Electrostatic charges calculated on a dimeric unit in P3TzT using the RB3LYP method and 6-31G (D) basis set are also consistent with the observation that 1,2,3-triazole behaves as an electron donor (see Supporting Information).

P3TzT was treated with trifluoroacetic acid (TFA) to protonate the nitrogen on the triazole moiety and decrease the electron-donating nature of triazole. After the addition of TFA, the absorption and emission λ_{max} of P3TzT, as expected, are blue-shifted by 20 and 21 nm, respectively. Cyclic voltammetry after addition of TFA indicates that the energy of the HOMO level is lowered and LUMO^{elec} is increased in energy, thus increasing the band gap (E_g^{elec}). All the above observations indicate that 1,2,3-triazole when attached as a pendant group to a thiophene backbone acts as an electron-donating group, pushing both the HOMO and LUMO levels up in energy and reducing the band gap. The triazole moiety does not hinder the packing of the polymer backbone in thin films.

Fluorescence Quenching with PCBM. To demonstrate that P3TzT polymer is a potential candidate for photovoltaic

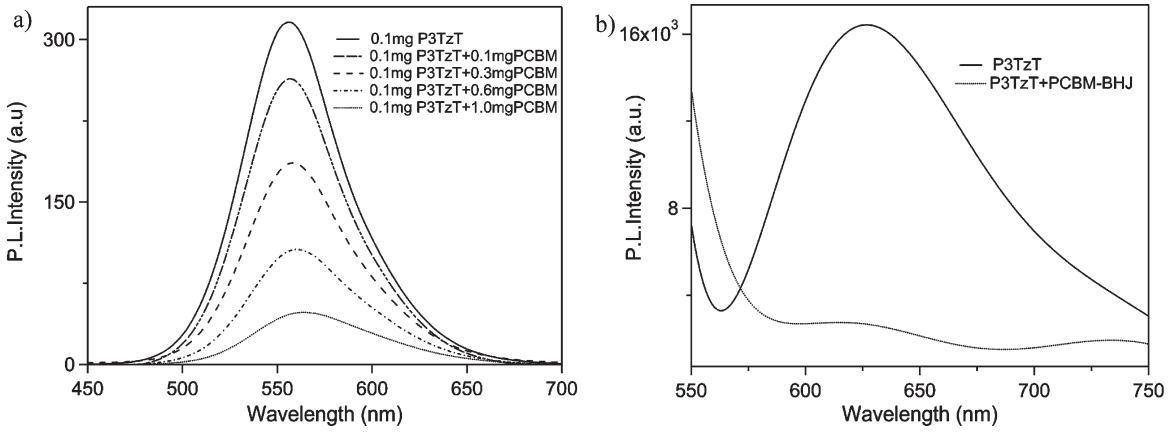

Figure 4. (a) Increase in fluorescence quenching by the addition of more PCBM (in chloroform). (b) Complete fluorescence quenching in the thin film of P3TzT and PCBM.

applications, fluorescence quenching studies with varying weight ratios of PCBM were carried out and are shown in Figure 4. The fluorescence intensity of P3TzT polymer was observed to decrease gradually with the increase in the weight ratio of PCBM, indicating the electron transfer from P3TzT to PCBM and hence fluorescence quenching. Thin films casted onto a glass plate from chloroform solution containing 1:1 wt % P3TzT and PCBM did not exhibit any fluorescence, indicating complete fluorescence quenching. Thus, the above observations indicate that P3TzT is a potential candidate for applications in photovoltaic devices.

Conclusions

We have shown that the thiophene-based polymers with 1,2,3-triazole moiety attached as a pendant group can be synthesized using Ni(0)-mediated Grignard metathesis polymerization using a modified monomer. When compared with a triazole on the main chain, the pendant triazole moiety acts as an electron donor and lowers the band gap of the polymer. The triazole moiety also does not hinder the packing of the conjugated backbone. We have also shown that the fluorescence of this polymer is quenched with PCBM, indicating its potential as a candidate for organic PV devices. Efforts are underway to evaluate the hole mobilities and photovoltaic metrics of thiophene-based polymers with pendant triazole moiety and will be reported in due course.

Acknowledgment. We thank the Energy Frontier Research Center supported by the US Department of Energy, Office of Basic Energy Sciences, through Grant DE-SC0001087 and the NSF Materials Research Science and Engineering Center at the University of Massachusetts Amherst for financial support. We also thank Ms. Dian Chen for her help in recording X-ray powder diffraction patterns.

Supporting Information Available: Synthetic procedures and characterization data for the monomers, synthetic procedures and characterization data for the polymers, details about electrostatic charge calculation on the dimer, and powder X-ray diffraction patterns of the polymers. This material is available free of charge via the Internet at http://pubs.acs.org.

References and Notes

(1) Park, J. W.; Lee, D. H.; Chung, D. S.; Kang, D. M.; Kim, Y. H.; Park, C. E.; Kwon, S. K. *Macromolecules* **2010**, *43*, 2118–2123.
(2) Yu, C. Y.; Ko, B. T.; Ting, C.; Chen, C. P. *Sol. Energy Mater. Sol. Cells* **2009**, *93*, 613–620.
(3) Zou, Y. P.; Sang, G. Y.; Wu, W. P.; Liu, Y. Q.; Li, Y. F. *Synth. Met.* **2009**, *159*, 182–187.
(4) He, Y. J.; Wu, W. P.; Liu, Y. Q.; Li, Y. F. *J. Polym. Sci., Part A-1: Polym. Chem.* **2009**, *47*, 5304–5312.
(5) Huang, F.; Chen, K. S.; Yip, H. L.; Hau, S. K.; Acton, O.; Zhang, Y.; Luo, J. D.; Jen, A. K. Y. *J. Am. Chem. Soc.* **2009**, *131*, 13886–13887.
(6) Huo, L. J.; Tan, Z. A.; Wang, X.; Zhou, Y.; Han, M. F.; Li, Y. F. *J. Polym. Sci., Part A-1: Polym. Chem.* **2008**, *46*, 4038–4049.
(7) Shen, P.; Sang, G. Y.; Lu, J. J.; Zhao, B.; Wan, M. X.; Zou, Y. P.; Li, Y. F.; Tan, S. T. *Macromolecules* **2008**, *41*, 5716–5722.
(8) Tan, Z. A.; Zhou, E. J.; Yang, Y.; He, Y. J.; Yang, C. H.; Li, Y. F. *Eur. Polym. J.* **2007**, *43*, 855–861.
(9) Zou, Y. P.; Wu, W. P.; Sang, G. Y.; Yang, Y.; Liu, Y. Q.; Li, Y. F. *Macromolecules* **2007**, *40*, 7231–7237.
(10) Zhou, E. J.; He, C.; Tan, Z.; Yang, C. H.; Li, Y. F. *J. Polym. Sci., Part A-1: Polym. Chem.* **2006**, *44*, 4916–4922.
(11) Hou, J. H.; Huo, L. J.; He, C.; Yang, C. H.; Li, Y. F. *Macromolecules* **2006**, *39*, 594–603.
(12) Hou, J. H.; Yang, C. H.; Li, Y. F. *Synth. Met.* **2005**, *153*, 93–96.
(13) Hou, J. H.; Tan, Z. A.; Yan, Y.; He, Y. J.; Yang, C. H.; Li, Y. F. *J. Am. Chem. Soc.* **2006**, *128*, 4911–4916.
(14) Li, Y. F.; Zou, Y. P. *Adv. Mater.* **2008**, *20*, 2952–2958.
(15) Kolb, H. C.; Finn, M. G.; Sharpless, K. B. *Angew. Chem., Int. Ed.* **2001**, *40*, 2004–2021.
(16) Fournier, D.; Du Prez, F. *Macromolecules* **2008**, *41*, 4622–4630.
(17) Binder, W. H.; Sachsenhofer, R. *Macromol. Rapid Commun.* **2007**, *28*, 15–54.
(18) Benanti, T. L.; Kalaydjian, A.; Venkataraman, D. *Macromolecules* **2008**, *41*, 8312–8315.
(19) Zeng, Q.; Li, Z.; Li, Z.; Ye, C.; Qin, J.; Tang, B. Z. *Macromolecules* **2007**, *40*, 5634–5637.
(20) Bu, H. B.; Gotz, G.; Reinold, E.; Vogt, A.; Schmid, S.; Blanco, R.; Segura, J. L.; Bauerle, P. *Chem. Commun.* **2008**, 1320–1322.
(21) Englert, B. C.; Bakbak, S.; Bunz, U. H. F. *Macromolecules* **2005**, *38*, 5868–5877.
(22) Zheng, Q. D.; Jung, B. J.; Sun, J.; Katz, H. E. *J. Am. Chem. Soc.* **2010**, *132*, 5394–5404.
(23) Pommerehne, J.; Vestweber, H.; Guss, W.; Mahrt, R. F.; Bassler, H.; Porsch, M.; Daub, J. *Adv. Mater.* **1995**, *7*, 551–554.
(24) Sun, Q. J.; Wang, H. Q.; Yang, C. H.; Li, Y. F. *J. Mater. Chem.* **2003**, *13*, 800–806.
(25) Li, G.; Shrotriya, V.; Huang, J. S.; Yao, Y.; Moriarty, T.; Emery, K.; Yang, Y. *Nature Mater.* **2005**, *4*, 864–868.
(26) Dimitrakopoulos, C. D.; Malenfant, P. R. L. *Adv. Mater.* **2002**, *14*, 99–117.
(27) Huynh, W. U.; Dittmer, J. J.; Alivisatos, A. P. *Science* **2002**, *295*, 2425–2427.
(28) Sirringhaus, H.; Brown, P. J.; Friend, R. H.; Nielsen, M. M.; Bechgaard, K.; Langeveld-Voss, B. M. W.; Spiering, A. J. H.; Janssen, R. A. J.; Meijer, E. W.; Herwig, P.; de Leeuw, D. M. *Nature* **1999**, *401*, 685–688.
(29) Bao, Z.; Dodabalapur, A.; Lovinger, A. J. *Appl. Phys. Lett.* **1996**, *69*, 4108–4110.
(30) He, Y. J.; Chen, H. Y.; Hou, J. H.; Li, Y. F. *J. Am. Chem. Soc.* **2010**, *132*, 1377–1382.
(31) Zhao, G. J.; He, Y.; Li, Y. F. *Adv. Mater.* **2010**, DOI: 10.1002/adma.201001339.
(32) Klapars, A.; Buchwald, S. L. *J. Am. Chem. Soc.* **2002**, *124*, 14844–14845.
(33) Loewe, R. S.; Khersonsky, S. M.; McCullough, R. D. *Adv. Mater.* **1999**, *11*, 250–253.
(34) Iovu, M. C.; Sheina, E. E.; Gil, R. R.; McCullough, R. D. *Macromolecules* **2005**, *38*, 8649–8656.
(35) Pretsch, E.; Buhlmann, P.; Affolter, C. In *Structure Determination of Organic Compounds*, 3rd ed.; Springer: Berlin, 2000; p 186.
(36) Koeckelberghs, G.; Vangheluwe, M.; Van Doorsselaere, K.; Robijns, E.; Persoons, A.; Verbiest, T. *Macromol. Rapid Commun.* **2006**, *27*, 1920–1925.
(37) Amarasekara, A. S.; Pomerantz, M. *Synthesis* **2003**, 2255–2258.
(38) Boyd, S. D.; Jen, A. K. Y.; Luscombe, C. K. *Macromolecules* **2009**, *42*, 9387–9389.
(39) Loewe, R. S.; Ewbank, P. C.; Liu, J. S.; Zhai, L.; McCullough, R. D. *Macromolecules* **2001**, *34*, 4324–4333.
(40) Zhou, Z.; Fahrni, C. J. *J. Am. Chem. Soc.* **2004**, *126*, 8862–8863.
(41) Parent, M.; Mongin, O.; Kamada, K.; Katan, C.; Blanchard-Desce, M. *Chem. Commun.* **2005**, 2029–2031.
(42) Bundgaard, E.; Krebs, F. C. *Sol. Energy Mater. Sol. Cells* **2007**, *91*, 954–985.
(43) Ajayaghosh, A. *Chem. Soc. Rev.* **2003**, *32*, 181–191.
(44) Zeng, G.; Chua, S. J.; Huang, W. *Thin Solid Films* **2002**, *417*, 194–197.
(45) Bredas, J. L.; Heeger, A. J. *Chem. Phys. Lett.* **1994**, *217*, 507–512.
(46) Yasuda, T.; Namekawa, K.; Iijima, T.; Yamamoto, T. *Polymer* **2007**, *48*, 4375–4384.
(47) Yasuda, T.; Imase, T.; Sasaki, S.; Yamamoto, T. *Macromolecules* **2005**, *38*, 1500–1503.